We are IntechOpen, the world's leading publisher of Open Access books Built by scientists, for scientists

4,800
Open access books available

122,000
International authors and editors

135M
Downloads

Our authors are among the

154
Countries delivered to

TOP 1%
most cited scientists

12.2%
Contributors from top 500 universities

CLARIVATE ANALYTICS BOOK CITATION INDEX INDEXED

WEB OF SCIENCE™

Selection of our books indexed in the Book Citation Index in Web of Science™ Core Collection (BKCI)

Interested in publishing with us?
Contact book.department@intechopen.com

Numbers displayed above are based on latest data collected.
For more information visit www.intechopen.com

14

Curing Monitoring of Composite Material Using Embedded Fiber Bragg Grating Sensors

Chia-Chin Chiang
Department of Mechanical Engineering, National Kaohsiung University of Applied Sciences, 415 Chien Kung Road, Kaohsiung 807, Taiwan

1. Introduction

The composite materials with high specific stiffness and strength have been widely applied in various fields such as aerospace or industry. Simultaneously, curing methods for joining composite materials have also gone through development intensively, for examples Hot-press, Pultrusion, Resin Transfer Molding (RTM) and Vacuum Molding. During the curing process, internal damages and residual strain are the most considerable relevance to quality of product, and hence demanded careful treatment. Commonly, the internal damage of composite materials could be detected by using ultrasound scan and X-ray, but these methods, however, are significantly high cost and not on-line monitoring. It is not suitable for smart structure application.

Since several recent decades, optical fiber sensors have been utilized in composite material field popularly for their predominating advantages such as small size, low cost, and capability of avoiding electromagnetic influence. In 1988, Afromowitz proposed the polymer fiber embedded into composite materials to monitor the refractive index changes in the composite materials during curing process [Afromowitz, 1988]. And one year later the authors presented Fiber Optic Fresnel Reflection Technique for supervising the curing process [Afromowitz & Lam, 1990]. In late 1980s, Fiber Bragg Grating (FBG) sensor, one kind of optical fiber sensors, has attracted considerable attentions to the applications in aerospace, structural, medical and chemical spheres. FBG sensors are small and compatible with common polymeric materials, and thereby being easily embedded close to the internal sensing site in a composite structure without introducing significant defects.

In 1990, Dunphy et al. employed the Fiber Bragg Grating embedded into composite materials to monitor the vitrification during curing process [Dunphy et al., 1990]. Similarly, FBG sensors were also applied to measure strain and residual stress after curing [Dewynter-Marty et al., 1998 & Okabe et al., 2002a]. On the other hand, Kuang and collegues improved detecting effect of the sensors by embedding FBG into composite materials in different layers [Kuang et al., 2001b]. Alternatively, in 2002, Okabe et al. utilized small-diameter FBG to study residual stress with micro damage of inner structure of the composite [Okabe et al., 2002b]. Furthermore, FBG has been also used to monitor the epoxy curing, and found the glass transition temperature with intensity changes [Giordano et al., 2004 & Wang et al., 2007].

Recent studies [Okabe et al., 2002a & Kuang et al., 2001a] discovered that when FBG sensors are embedded in CFRP laminates, the reflection spectrum from the sensors splits into two peaks because of the non-axisymmetric thermal residual stresses. This deformation of the spectrum was considered defective as it would lead to misinterpretation in strain measurements or crack detection in the laminates [Menendez & Guemes, 2000; Murukeshan et al., 2000; Leng & Asundi, 2002].

According to our knowledge, most of the previous researches focus on measuring the mechanical properties of composite materials and damage evaluation, but lack of curing residual strain monitoring in different layers. The aim of current study is to apply Fiber Bragg Grating sensors to monitor the characteristics of the curing process in a Graphite/Epoxy composite. Four FBGs are embedded into different lamina of composite materials, and the curing development as well as internal residual strain during curing process would be measured.

2. Theory

2.1 Fiber Bragg Grating Sensor

Fiber Bragg Grating Sensor consists of thousands of short period refractive index modulation. When the broad band light source lunches at the FBG, the certain wavelength of the light will be reflected. The reflected wavelength of FBG can be expressed as following [Hill & Meltz, 1997]:

$$\lambda = 2n_{eff}\Lambda \tag{2-1}$$

where n_{eff} is the effective refractive index of optical fiber, Λ is the grating period which is about 1um. Fig. 1 illutrates the principle of FBG schematically.

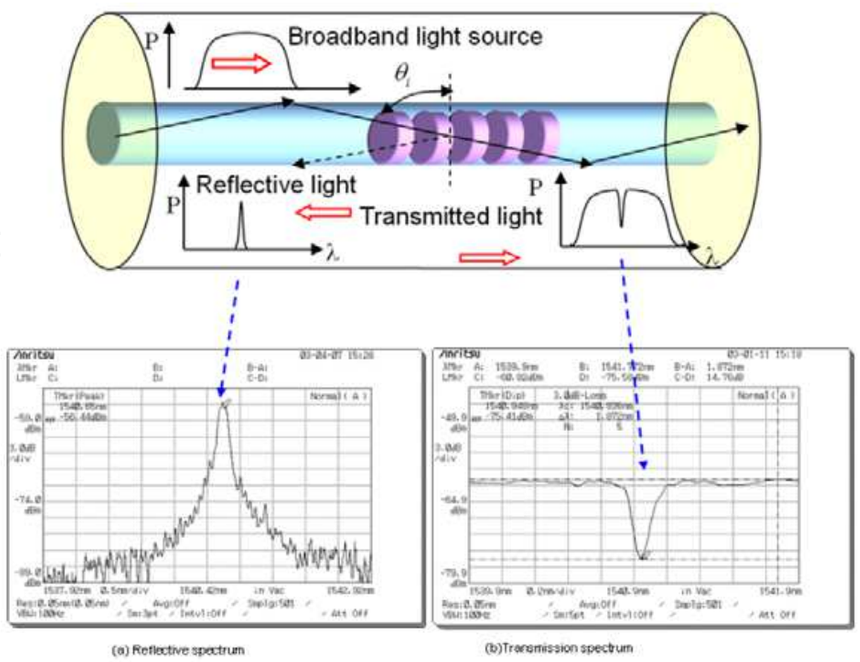

Fig. 1. Reflective and transmission spectra of single-mode fiber Bragg gratings

2.2 FBG wavelength shifts owing to temperature and strain

Because of thermo-optic effect and Photo-Elastic effect, the wavelength of FBG will be shifted with changes of temperature and strain. The FBG wavelength is a function of the temperature and strain and in form as following [Hill & Meltz, 1997]:

$$\frac{\Delta\lambda}{\lambda} = \left\{1 - \frac{n_{eff}^2}{2}\left[p_{12} - \nu\left(p_{11} - p_{12}\right)\right]\right\}\varepsilon + \left[\alpha + \frac{\left(\frac{dn_{eff}}{dT}\right)}{n_{eff}}\right]\Delta T$$
$$= \left(1 - p_e\right)\varepsilon + \left(\alpha + \xi\right)\Delta T = K_\varepsilon \varepsilon + K_T \Delta T \tag{2-2}$$

where ξ is the thermo-optical coefficient, α is the CTE of optical fiber, ΔT is the temperature change, K_ε is the strain sensitivity, and K_T is the temperature sensitivity.

2.3 FBG spectrum splitting with residual strain

Theoretically, the wavelength of FBGs shifted under two strain conditions including uniaxial and multiaxial strain. Following, discussion about the two kinds of wavelength shift is presented particularly.

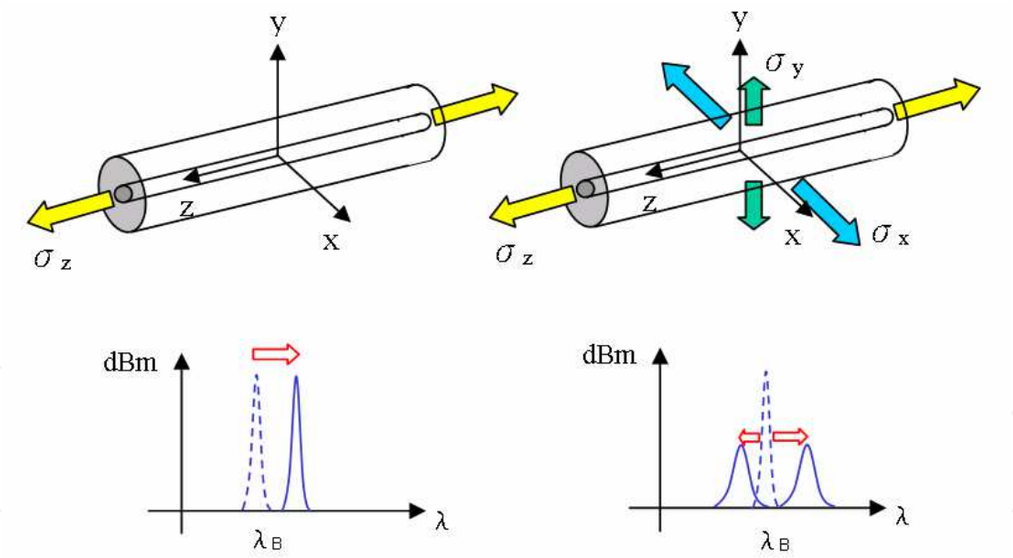

(a) (b)

Fig. 2. The optical fiber Bragg grating sensor is under an uniaxial strain (a) and a general multiaxial strain (b). [Lin, 2004]

(I) Wavelength shift due to uniaxial strain

When the fiber is suffered a uniaxial uniform strain ε_i along its axis (as shown in Fig. 2a), then $\varepsilon_x = \varepsilon_y = -\nu\varepsilon_z$ (ν is the Poisson ratio of optical fiber). As a result, the wavelength shift is related to the applied strain and temperature change as given by equations below:

$$\frac{\Delta\lambda_B}{\lambda_B} = K_\varepsilon \varepsilon \ + K_T \Delta T \tag{2-3}$$

where $K_T = \frac{\xi}{n_0} + [1 - \frac{n_0^2}{2}(p_{11} + p_{12})]\alpha$, $K_\varepsilon = 1 - \frac{n_0^2}{2}[p_{12} - (p_{11} + p_{12})]$.

Referring to work [Lin, 2004], p_{11} =0.113, p_{12} =0.252, and $n_{eff,0}$ ~1.458, ν ~0.17, α ~0.55×10^{-6}, one can obtain the constants K_ε ~0.8 and K_T ~5.88×10^{-6}. The strain is measured by the reflective wavelength shift of the fiber Bragg gratings.

(II) Wavelength shift due to multiaxial strain

When the FBGs are embedded in the composite laminate, the FBG will be suffered three dimensional loading. As the fiber is under a general multiaxial strain (Fig. 2 b), the Bragg wavelength shifts caused by refractive index changes in the x- and y- directions are dissimilar. As shown in the Fig. 2 b, the original Bragg reflection peak is shifted in two opposite directions, and thereby causing spectra to split [Lin, 2004]. This phenomenon is due to the birefringence effect.

The 3-D strain and wavelength effect is shown as following [Lin, 2004; Menendez & Guemes, 2000]:

$$\begin{Bmatrix} \frac{\Delta\lambda_x}{\lambda_x} \\ \frac{\Delta\lambda_x}{\lambda_x} \end{Bmatrix} = \begin{bmatrix} D_1 & D_2 \\ D_1 & D_3 \end{bmatrix} \begin{Bmatrix} \varepsilon_x \\ \varepsilon_y \end{Bmatrix} + K_T \Delta T \{I\} \tag{2-4}$$

where D_1, D_2 and D_3 are constant. $D_1 = 1 + \frac{n_0^2}{2}[\upsilon(p_{11} + p_{12}) - p_{12}]$, $D_2 = -\upsilon + \frac{n_0^2}{2}[2\upsilon p_{12} - p_{11}]$, $D_3 = -\upsilon + \frac{n_0^2}{2}[\upsilon(p_{11} + p_{12}) - p_{12}]$, $K_T = \frac{\xi}{n_0} + [1 - \frac{n_0^2}{2}(p_{11} + 2p_{12})]\alpha$, and $\{I\}$ is the unit matrix.

Therefore, the curing residual strain can be monitoring according to the spectra of the embedded FBGs. The Residual strain along the x-axial and y-axial are expressed in following [Menendez & Guemes, 2000]:

$$\varepsilon_y = \frac{\frac{\Delta\lambda_y}{\lambda_y} - \frac{\Delta\lambda_z}{\lambda_z}}{D_2 - D_3} \tag{2-5}$$

$$\varepsilon_x = \frac{1}{D_1}\left\{\left[\frac{\left(\frac{\Delta\lambda_y}{\lambda_y} - \frac{\Delta\lambda_z}{\lambda_z}\right)D_3}{D_2 - D_3}\right] - \frac{\Delta\lambda_z}{\lambda_z}\right\} \tag{2-6}$$

By monitoring the 3-dimemsional strain in the composite laminate, we can measure and evaluate the curing residual strain during the process.

3. Experimental results

3.1 Preparation of the composite laminate

The 16-layer thermosetting prepregs, Carbon/Epoxy composition T300/3501, are used for laying up the composite laminate in the sequence with four embedded FBGs [0(FBG-1)90/0(FBG-2)90/0(FBG-3)90/0(FBG-4)0/90/0/90/0/90/0/90/0]. The curing process is implemented by utilizing the Modified Diaphragm Forming (MDF) with the air compressor, vacuum pump, and heat chamber. The mod of MDF consists of two Teflon films to prevent adhesion, polyimide-diaphragm and o-ring for sealing, which is depicted in Fig. 3.

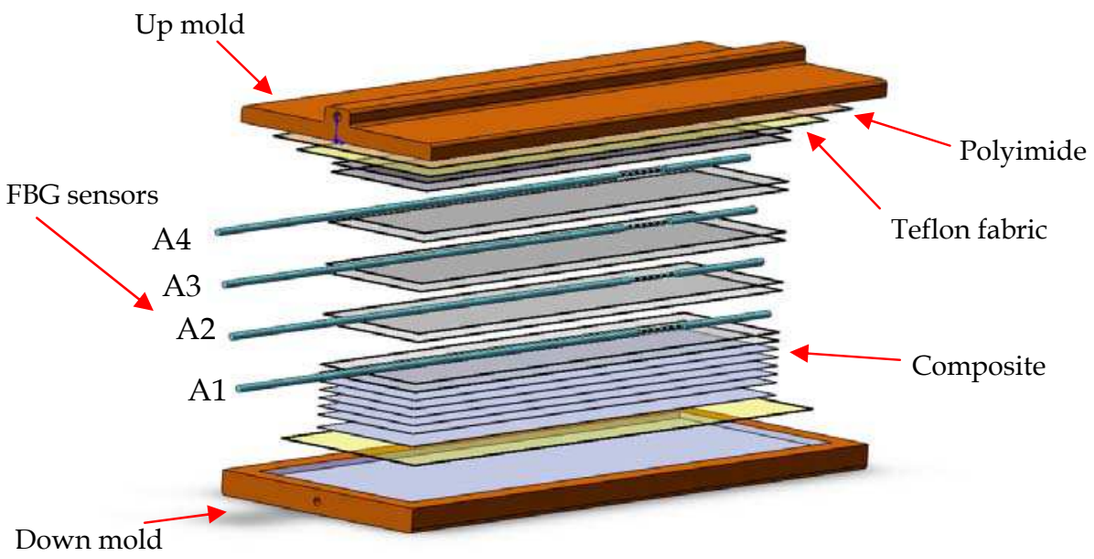

Fig. 3. Schematic of the diaphragm type forming mold for laminate curing process

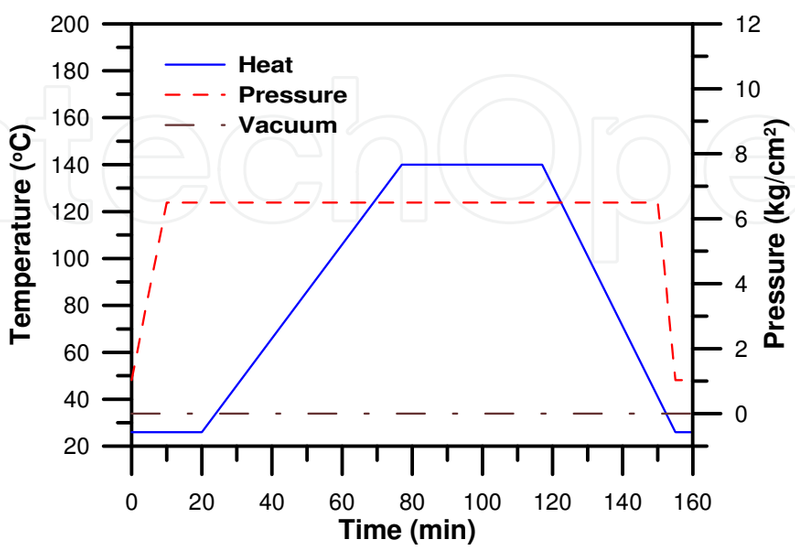

Fig. 4. Curing conditions of composite specimen

The prepregs in MDF will be closed by air pressure beyond the diaphragm, and removed excess gas in the laminate by vacuum pump simultaneously. The curing process is composed of three stages including heating, isothermal and cooling stage. The process starts at heating stage with 7 kg/cm² air pressure upon the diaphragm, and 6.5 kg/cm² vacuum in the mod. The heating rate is 2 °C/min from room temperature to 140 °C. Second state is isothermal stage at 140 °C in 40mins. During this stage, the resin viscosity is low and easy to flow. The vacuum condition assists avoiding the delamination due to the exhaust gas in the laminate. The third state is cooling to room temperature when the resin viscosity becomes large and stable. Moreover, the residual strain will occur at the end of this stage. The whole curing conditions are described in Fig. 4.

3.2 Experimental set-up and fabrication of FBG

The involved FBG was fabricated in the Ge-B co-doped single cladding photosensitive fiber by using the phase mask method. Meanwhile, the photosensitive fiber was manufactured by Fibercore Co. Ltd. (PS1250/1550).

A schematic diagram of photoimprinting FBGs in photosensitive optical fiber is illustrated in Fig. 5 particularly. The 248-nm UV radiation from a KrF Excimer laser is employed while the impulse frequency of laser is 10 Hz. To avoid burning the phase mask, the laser power should be <500 mJ/cm². Along the fiber core, the FBG has a periodic refractive index modulation with a period of 1.05~1.08 μm, obtained by using phase masks with different periods. This resulted in a peak Bragg reflecting wavelength of 1540~1564 nm. The reflectivity of the resulting FBG was about 99% and the FWHM (Full width Half Maximum) of the FBG is about 0.175 nm.

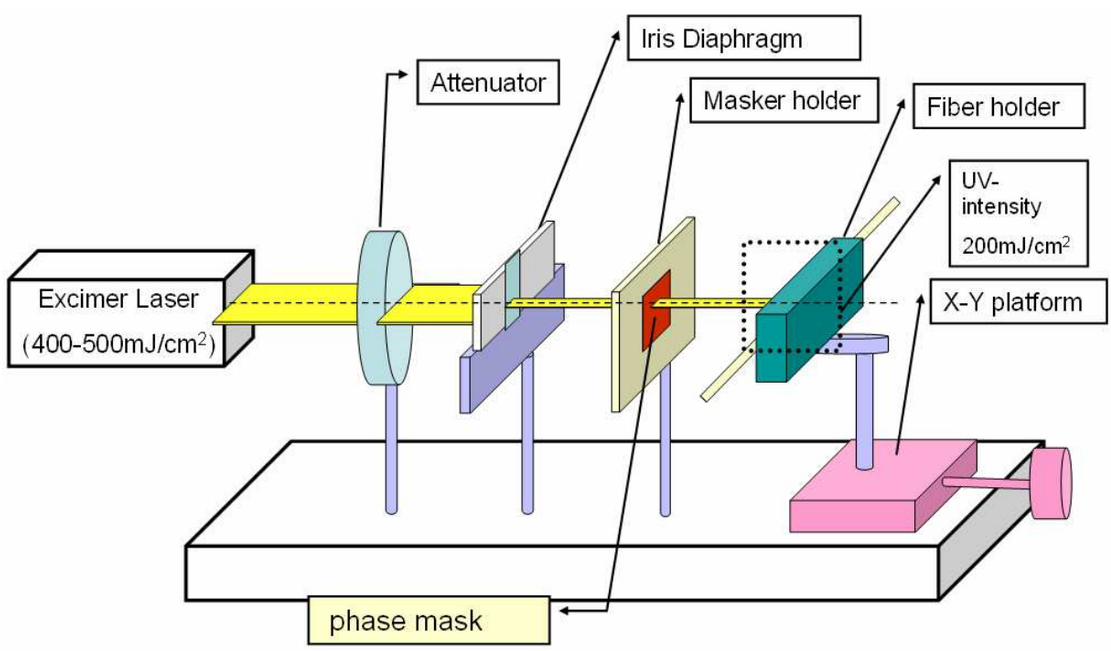

Fig. 5. A schematic diagram of the FBGs fabrication set-up

The experimental set-up for curing monitoring is shown in Fig. 6. The light source in the experiment is the broadband Super Luminescent Diode (SLED) with wavelength span is

1400nm~1600nm. The main objective of the system is to observe the reflective spectra from the embedded FBGs in the laminate.

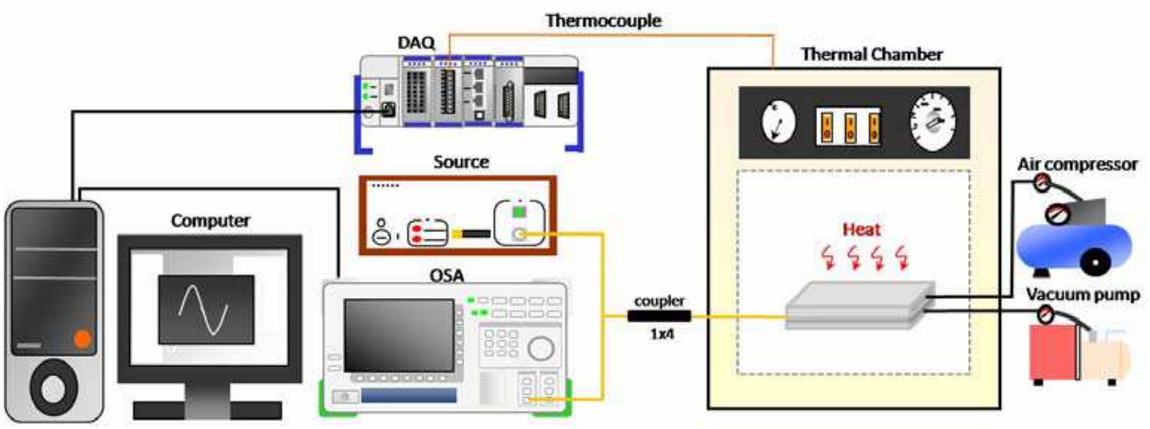

Fig. 6. Experimental set-up of curing monitoring

3.3 Results and discussion

We embedded four FBGs (FBG-A1:1541.13nm, FBG-A2:1552.85nm, FBG-A3:1554.61nm, and FBG-A4:1560.65nm) into the composite laminate. Fig. 7 depicts the temperature calibration (from room temperature to 180 °C) of FBGs before embedded in the laminate. The temperature sensitivity of FBG-A1, FBG-A2, FBG-A3 and FBG-A4 are 9.8, 9.5, 11.4 and 9.4, respectively. It could be observed that the variation of wavelength with temperature is quite linear with the average of R-squared is 0.997.

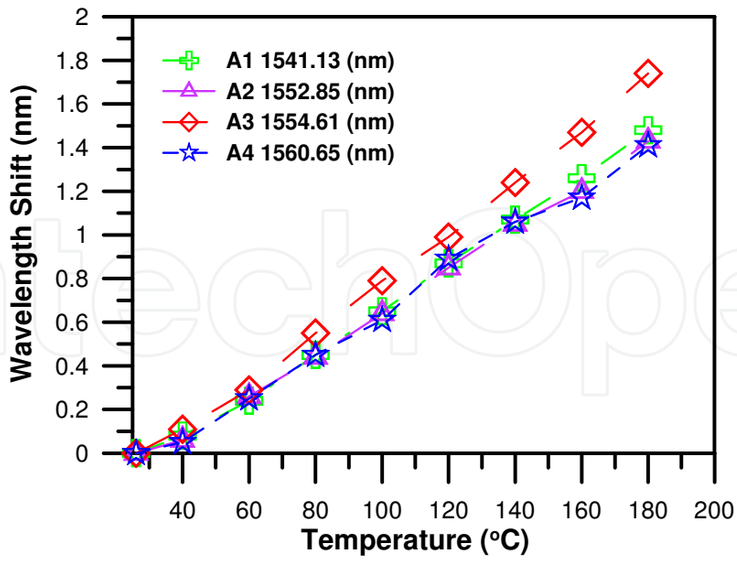

Fig. 7. FBG wavelength shift with the temperature raising

From the reflective spectrum of embedded FBG sensors, we can observe the peak wavelength of FBGs (FBG-A1:1540.81nm, FBG-A2:1552.6nm and FBG-A3:1554.79nm). The signal of FBG-A4 is very weak after raising the air pressure in the up-mod. The high

pressure could be the reason causing the breakage of FBG-A4. As shown in Fig. 8, which describes the change of spectra and the intensity in the heating stage of the curing process, the wavelength shifts to the right while intensity is increasing with temperature rising. The phenomenon is as a result of the diminished compression loading. As the temperature increases, the viscosity of the matrix materials (Epoxy) is decreasing gradually. Therefore, the embedded FBG will be adapted well in the carbon fiber lamina. The pressure loading will be then taken by the carbon fiber, and thereby reducing the loading on the embedded FBGs. In the Fig. 9, there are three transition points of the intensity-temperature curve at about 105 °C, which is near to the glass transition temperature of the epoxy matrix (95 °C).

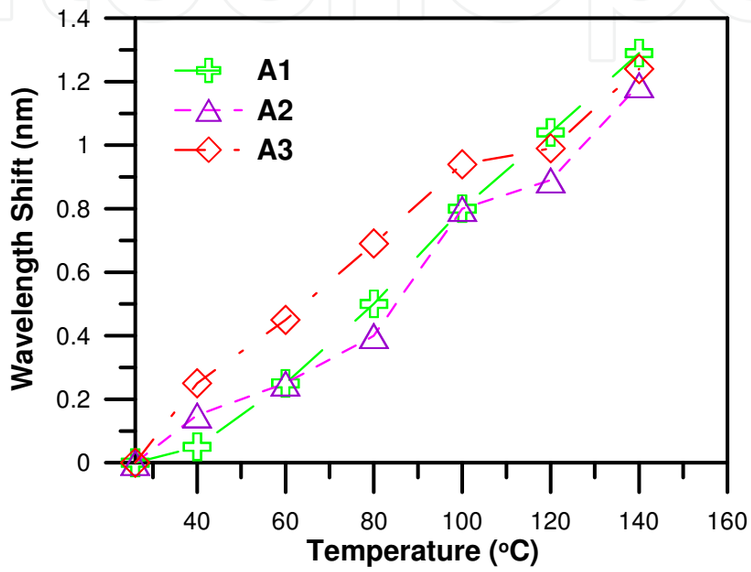

Fig. 8. FBG wavelength shift during heating stage during curing process

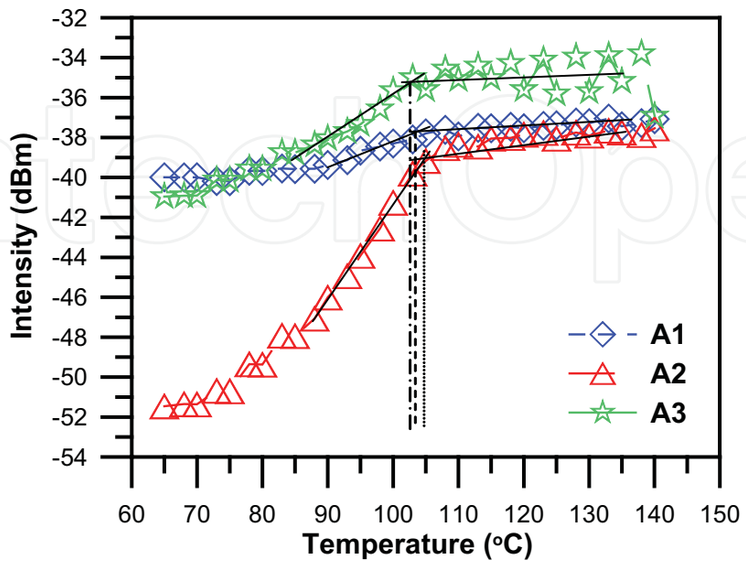

Fig. 9. The intensity changes of the embedded FBGs during the heating stage

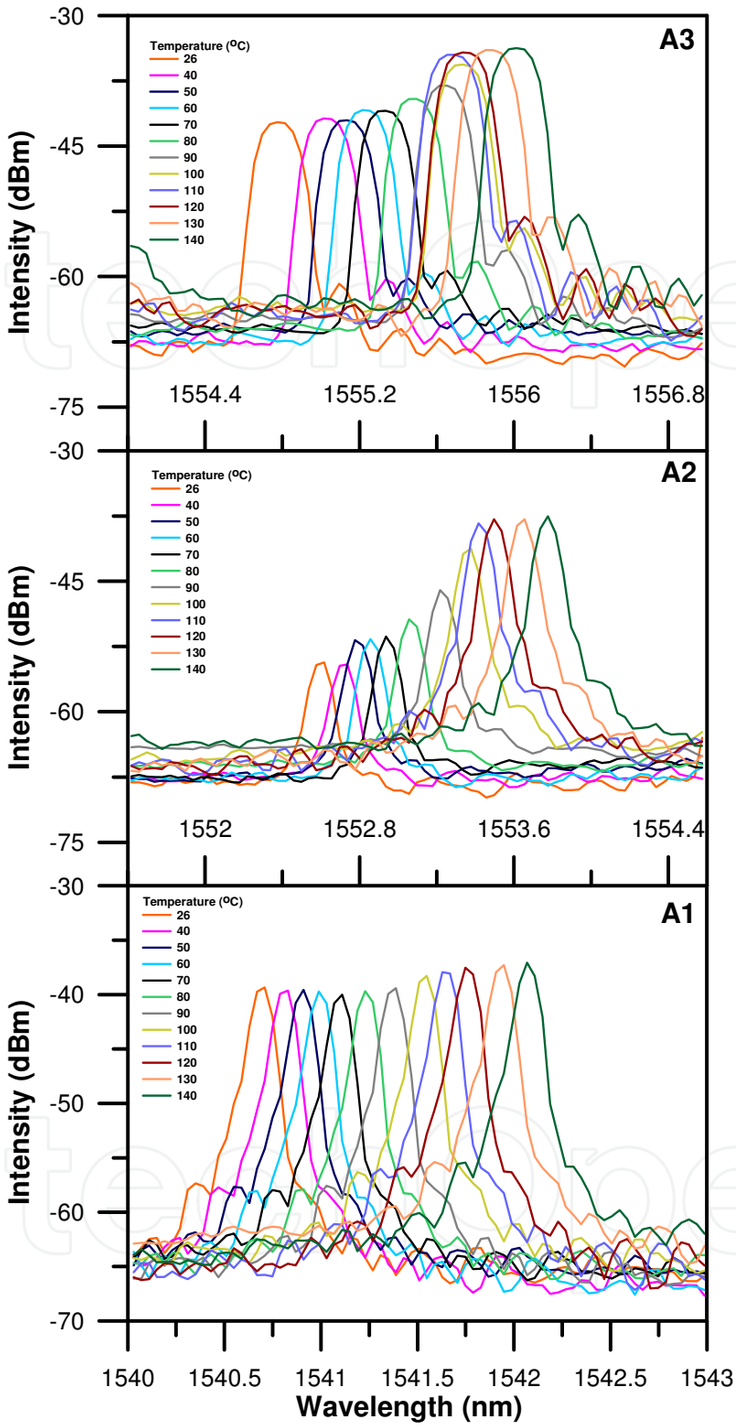

Fig. 10. Spectrum of change during the heating stage

The intensity and the spectrum shape of the FBGs do not change at the isothermal stage (holding at 140 °C). However, the resin viscosity is reducing gradually during cooling process. In cooling stage, the intensity of the embedded FBGs' spectra is linearly decreasing, and the spectrum width of FBGs is broadening with temperature cooling in Fig 10.

Fig. 11. illustrates the split of FBG spectra during cooling stage when the wavelength is shifted to left. The peak of FBG spectra (A1 and A2) gradually broadens at about 95 °C, and splitting into two peaks at 90 °C while the peak of FBG spectra (A3) broadens and splitting into two peaks at 50 °C.

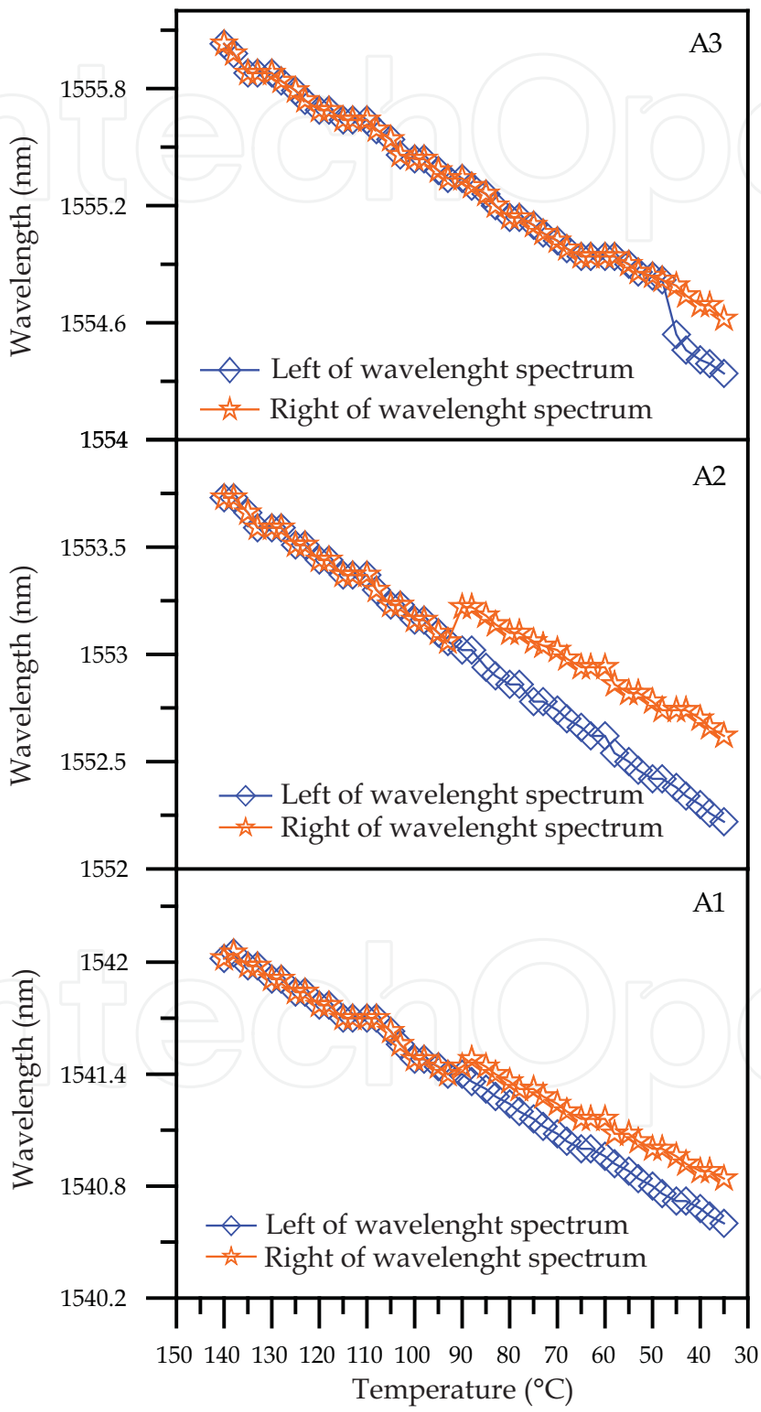

Fig. 11. The split of FBG spectra during the cooling stage

Fig. 12. depicts the variations of the intensity of FBG spectra during cooling stage. Below 90 °C, the spectra will split into two peaks, and, therefore, the intensity is decreasing with the occurrences of peak splitting.

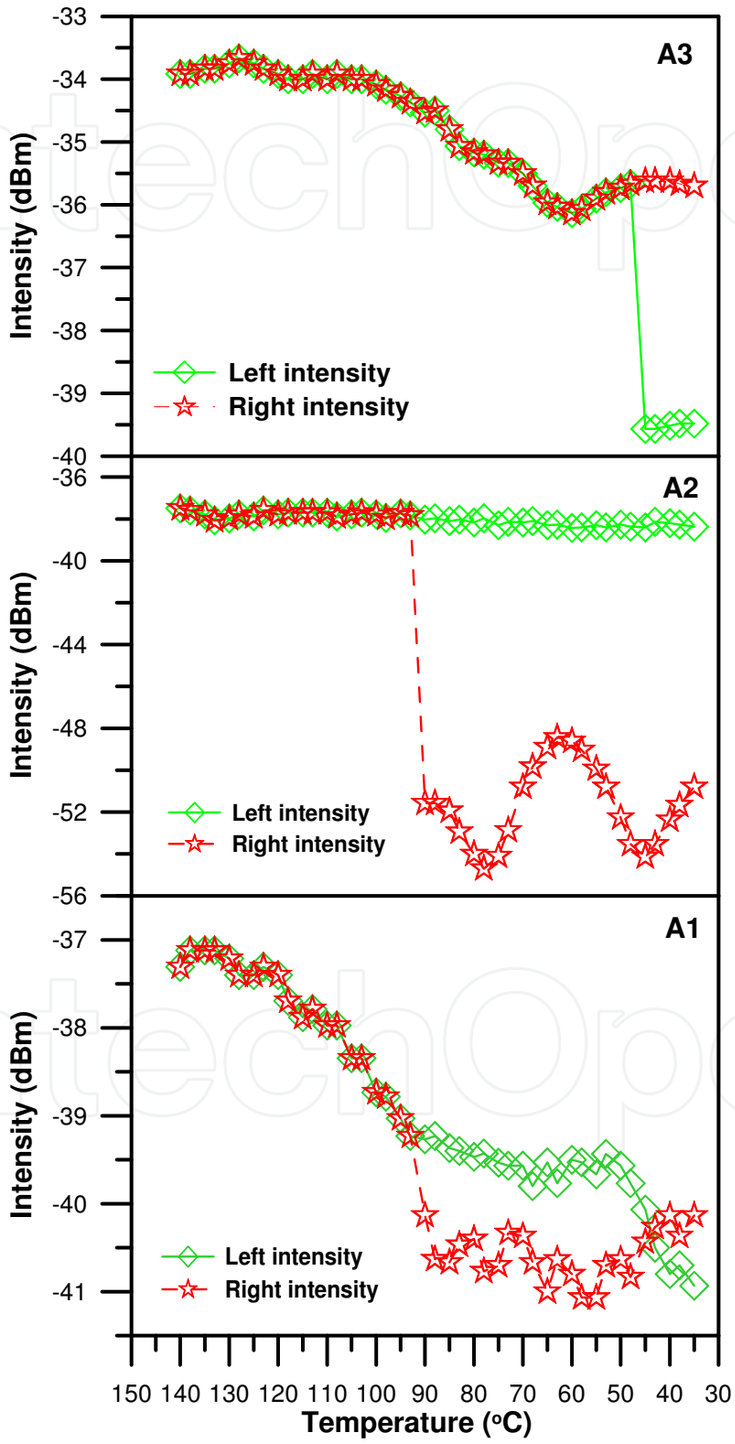

Fig. 12. Intensity of FBG Spectra during cooling stage

During the cooling process, we can observe the changes of intensity and wavelength in the FBGs' spectra. As shown in Fig. 13, the width of FBG spectra broadens below 100 °C. The spectra of FBG (A1 and A2) split into two peaks at about 90 °C whereas FBG (A3) splits at about 50 °C. In addition, splitting peaks of FBG (A3) are unobvious, and owing to smaller residual strain. This phenomenon may be caused by various residual strains from different layers of the laminated composites.

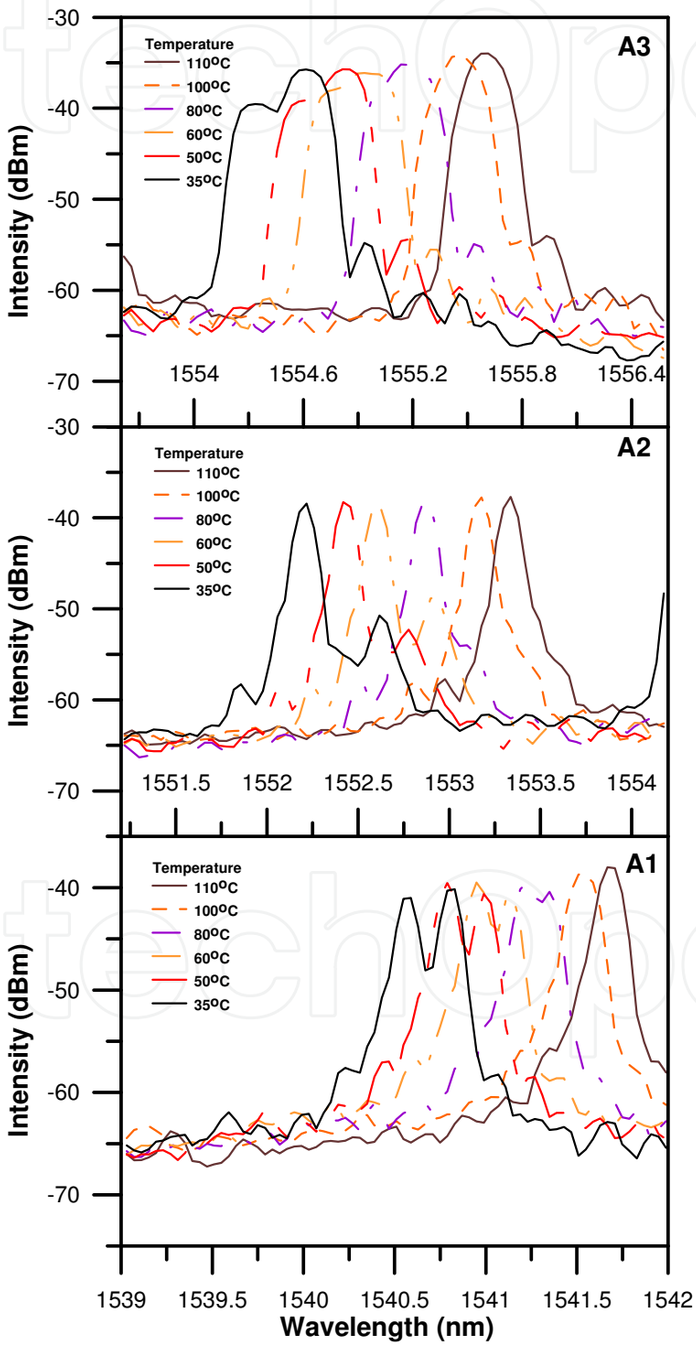

Fig. 13. FBG spectra monitoring during cooling stage

The comparison of the FBG spectra at before and after the curing process is illustrated in Fig. 14. After curing process, the spectra are shifted to left and splitting into two peaks owing to the transverse residual strain while the wavelengths of FBG (A1) and FBG (A2) shift to the left apparently. The wavelength shift is caused by the axial residual strain.

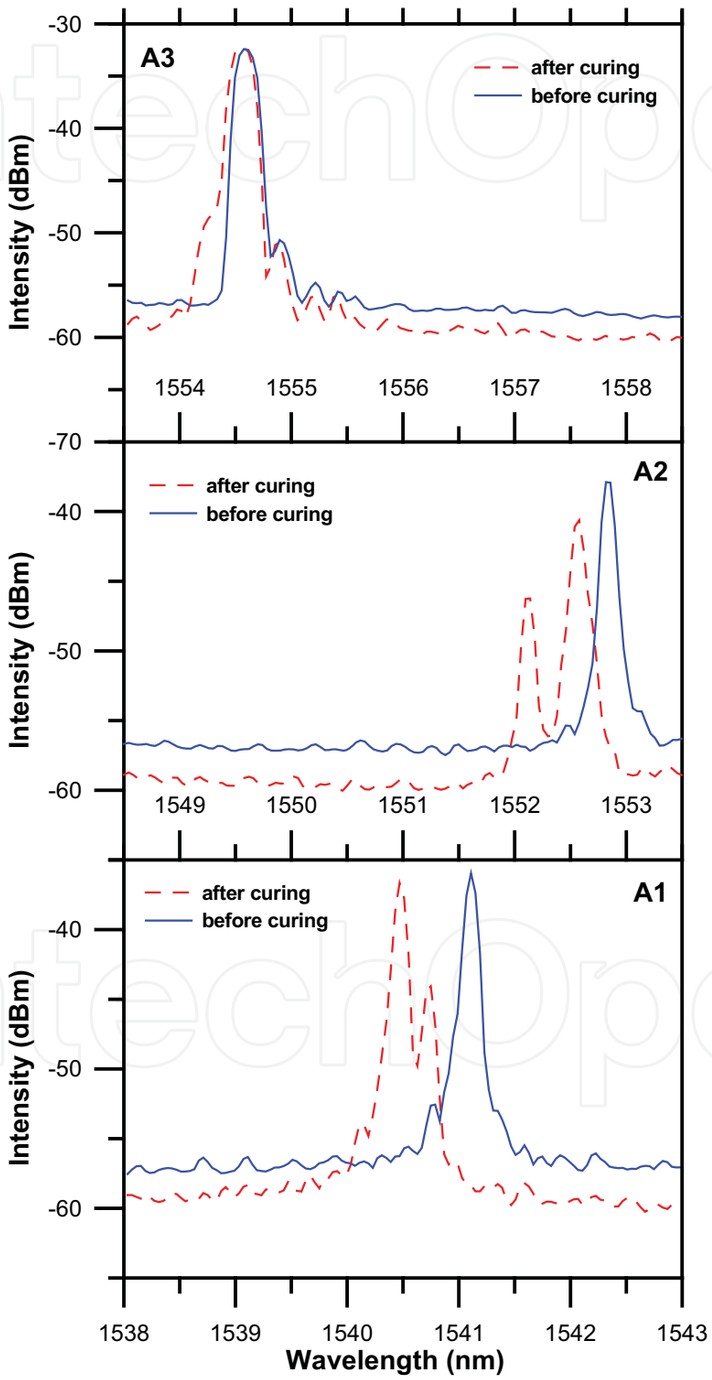

Fig. 14. Comparison of FBG spectra before and after curing

As shown in Fig.15, the residual strain of the FBG (A1) and FBG (A2) are -423με and -407με, respectively. Meanwhile, the residual strain of the FBG (A3) is -32με, much smaller than those of FBG (A1) and FBG (A2), could be considered as having no significant change after curing. Briefly, the residual strain of FBG (A1), FBG (A2) and FBG (A3) are compression strain although less residual strain could be detected at the outer layer of composite.

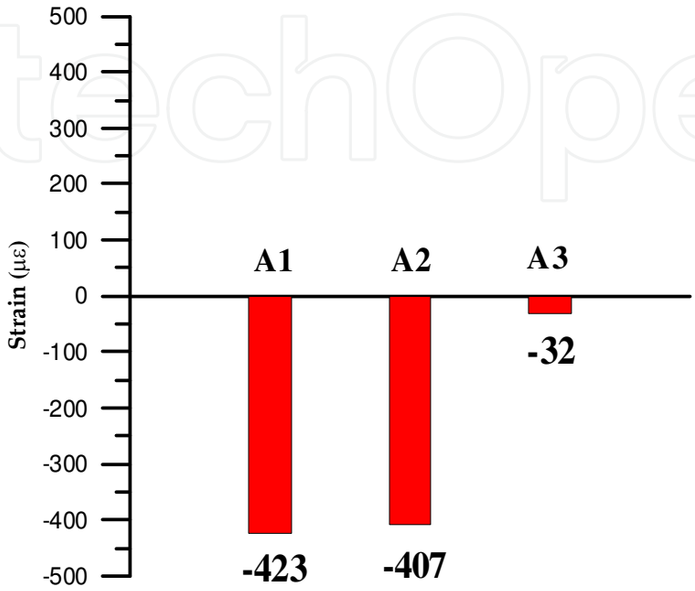

Fig. 15. Axis residual strain of FBG sensors in different layer of the composite laminate

5. Conclusions

We propose a method for monitoring the curing process of composite materials using four embedded FBGs in different layers in the composite laminate. The embedded FBGs are successful to supervise curing process including residual strain and glass transition temperature. The curing development and residual strain measurement are assessed through changes in the shape of the optical spectra, intensity attenuation and shifts in wavelengths of FBGs. The maximum curing residual strain was -423 με in the central laminate of the composite. The curing residual strain of FBG-1, FBG-2 and FBG-3 are -423, -407 and -32με, respectively. During the cooling stage, the spectra are shifted to left, broadening, and then splitting into two peaks owing to the transverse residual strain.

6. Acknowledgment

This work is supported by the National Science Council under contracts NSC 98-2221-E-151 -013 and NSC 99-2221-E-151-011.

7. References

Afromowitz, M. A. (1988). Fiber optic polymer cure sensor, *Journal of Lightwave Technology,* Vol. 6, No. 10, (August 2002), pp. (1591-1594), ISSN 0733-8724

Afromowitz, M. A. & Lam, K. Y. (1990). The optical properties of curing epoxies and applications to the fiber-optic epoxy cure sensor, *Sensors and Actuators A: Physical*, Vol. 23, No. 1-3, (April 1990), pp. (1107-1110), ISSN 0924-4247

Dewynter-Marty, V.; Ferdinand, P.; Bocherens, E.; Carbone, R.; Beranger, H.; Bourasseau, S.; Dupont, M. & Balageas, D. (1998). Embedded Fiber Bragg Grating Sensors for Industrial Composite Cure Monitoring, *Journal of Intelligent Material Systems and Structures*, Vol. 9, No. 10, (October 1998), pp. (785-787)

Dunphy, J. R.; Meltz, G.; Lamm, F. P. & Morey, W. W. (1990). Multifunction, distributed optical fiber sensor for composite cure and response monitoring, *Proceedings of Fiber Optic Smart Structures and Skins III*, San Jose, USA, September 1990

Giordano, M.; Laudati, A.; Nasser, J.; Nicolais, L.; Cusano, A. & Cutolo, A. (2004). Monitoring by a single fiber Bragg grating of the process induced chemo-physical transformations of a model thermoset, *Sensors and Actuators A: Physical*, Vol. 113, No. 2, (July 2004), pp. (166-173), ISSN 0924-4247

Hill, K. O. & Meltz, G. (1997). Fiber Bragg grating technology fundamentals and overview, *Journal of Lightwave Technology,* Vol. 15, No. 8, (August 2002), pp. (1263-1276), ISSN 0733-8724

Kuang, K. S. C.; Kenny, R.; Whelan, M. P.; Cantwell, W. J. & Chalker, P. R. (2001a). Residual strain measurement and impact response of optical fibre Bragg grating sensors in fibre metal laminates, *Smart Materials & Structures*, Vol. 10, No. 2, (April 2001), pp. (338-346), ISSN 0964-1726

Kuang, K. S. C.; Kenny, R.; Whelan, M. P.; Cantwell, W. J. & Chalker, P. R. (2001b). Embedded fibre Bragg grating sensors in advanced composite materials, *Composites Science and Technology*, Vol. 61, No. 10, (2001), pp. (1379-1387), ISSN 0266-3538

Lin, C.L. "Opto-Mechanical Applications of Microstructured Materials" PhD thesis, Joseph Fourier University /National Taiwan University, 2004.

Leng, J. S. & Asundi, A. (2002). Real-time cure monitoring of smart composite materials using extrinsic Fabry-Perot interferometer and fiber Bragg grating sensors, *Smart Materials & Structures*, Vol. 11, No. 2, (April 2002), pp. (249-255), ISSN 0964-1726

Menendez, J. M. & Guemes, J. A. (2000). Bragg-grating-based multiaxial strain sensing: its application to residual strain measurement in composite laminates, *Proceedings of Smart Structures and Materials 2000: Sensory Phenomena and Measurement Instrumentation for Smart Structures and Materials*, Newport Beach, CA, USA, March 2000

Murukeshan, V. M.; Chan, P. Y.; Ong, L. S. & Seah, L. K. (2000). Cure monitoring of smart composites using Fiber Bragg Grating based embedded sensors, *Sensors and Actuators A: Physical,* Vol. 79, No. 2, (February 2000), pp. (153-161), ISSN 0924-4247

Okabe, Y.; Yashiro, S.; Tsuji, R.; Mizutani, T. & Takeda, N. (2002a). Effect of thermal residual stress on the reflection spectrum from fiber Bragg grating sensors embedded in CFRP laminates, *Composites Part A: Applied Science and Manufacturing*, Vol. 33, No. 7, (July 2002), pp. (991-999), ISSN 1359-835X

Okabe, Y.; Mizutani, T.; Yashiro, S. & Takeda, N. (2002b). Detection of microscopic damages in composite laminates with embedded small-diameter fiber Bragg grating sensors,

Composites Science and Technology, Vol. 62, No. 7-8, (June 2002), pp. (951-958), ISSN 0266-3538

Wang, Y.; Han, B.; Bar-Cohen, A. & Cho, S. (2007). Fiber Bragg Grating Sensor to Characterize Curing Process-dependent Mechanical Properties of Polymeric Materials, *Proceedings of Electronic Components and Technology Conference, 2007. ECTC '07. Proceedings. 57th*, ISBN 0569-5503, June 2007

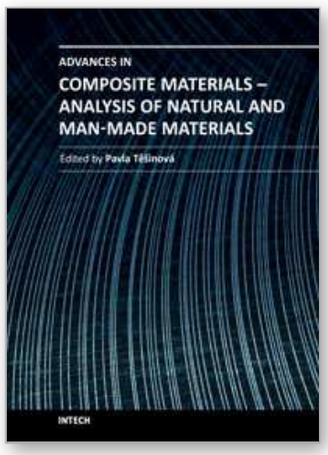

Advances in Composite Materials - Analysis of Natural and Man-Made Materials

Edited by Dr. Pavla Tesinova

ISBN 978-953-307-449-8
Hard cover, 572 pages
Publisher InTech
Published online 09, September, 2011
Published in print edition September, 2011

Composites are made up of constituent materials with high engineering potential. This potential is wide as wide is the variation of materials and structure constructions when new updates are invented every day. Technological advances in composite field are included in the equipment surrounding us daily; our lives are becoming safer, hand in hand with economical and ecological advantages. This book collects original studies concerning composite materials, their properties and testing from various points of view. Chapters are divided into groups according to their main aim. Material properties are described in innovative way either for standard components as glass, epoxy, carbon, etc. or biomaterials and natural sources materials as ramie, bone, wood, etc. Manufacturing processes are represented by moulding methods; lamination process includes monitoring during process. Innovative testing procedures are described in electrochemistry, pulse velocity, fracture toughness in macro-micro mechanical behaviour and more.

INTECH
open science | open minds

InTech Europe
University Campus STeP Ri
Slavka Krautzeka 83/A
51000 Rijeka, Croatia
Phone: +385 (51) 770 447
Fax: +385 (51) 686 166
www.intechopen.com

InTech China
Unit 405, Office Block, Hotel Equatorial Shanghai
No.65, Yan An Road (West), Shanghai, 200040, China
中国上海市延安西路65号上海国际贵都大饭店办公楼405单元
Phone: +86-21-62489820
Fax: +86-21-62489821

IntechOpen